

# Visual Attention for Rendered 3D Shapes

## Supplementary Material

Guillaume Lavoué<sup>1</sup>, Frédéric Cordier<sup>2</sup>, Hyewon Seo<sup>3</sup>, and Mohamed-Chaker Larabi<sup>4</sup>

<sup>1</sup>CNRS, Univ. Lyon, LIRIS, France

<sup>2</sup>University of Haute-Alsace, LMIA, France

<sup>3</sup>CNRS, University of Strasbourg, ICube, France

<sup>4</sup>CNRS, Univ. Poitiers, XLIM, UMR 7252, Poitiers, France

This supplementary material is organized as follows. Section 1 illustrates stimulus images/videos from the first experiment and Section 2 presents additional results from the first and second experiments. Section 3 details the mean AUC results for different threshold values and section 4 illustrates fixation maps and saliency maps for all images of the second experiment.

### 1. Stimuli from experiment 1

Figure 1 illustrates still image stimuli obtained with the Igea model with all materials and lighting conditions.

**9 videos files are also attached to this supplementary material** (in the *ExampleVideosWithHeatMaps* directory). They correspond to 9 video stimuli (downsampled and compressed) from the first experiment: the 3 objects with the 3 camera paths, for the top-left lighting and glossy material conditions.

### 2. Additional results

In this section, we first present the whole set of histograms that complete Figure 7 of the paper. They illustrate how disocclusions influence human fixations. Then we illustrate the effect of blurring on the global performance of saliency models (see Figure 3). We then provide additional per-class results: Linear correlations (see Figures 5 and 6) and AUC when saliency models are combined with center model (see Figure 4). We also provide per-objects Linear Correlation results (see Figures 7). Finally, Figure 8 details the p-values from the pairwise t-tests used in Figure 12 from the paper. Figure 9 details the same tests but conducted on the Linear Correlations instead of AUC values. Finally, Figure 10 details linear correlation values between fixation and Schelling distributions.

### 3. AUC results with different threshold values

As mentioned in Section 3.6 from the paper, to compute the AUC values the fixation maps are thresholded to obtain binary fixation maps. This threshold is chosen to have 20% of visible vertices being considered as fixations. To ensure that this threshold does not influence too much the metric, we provide in Figure 11, the AUC mean values of saliency models for different thresholds: 10%, 20%



**Figure 1:** Stimulus images of the Igea model obtained using the 3 materials and 3 lighting conditions.

and 40%. As can be seen, this parameter only has a slight influence on the results.

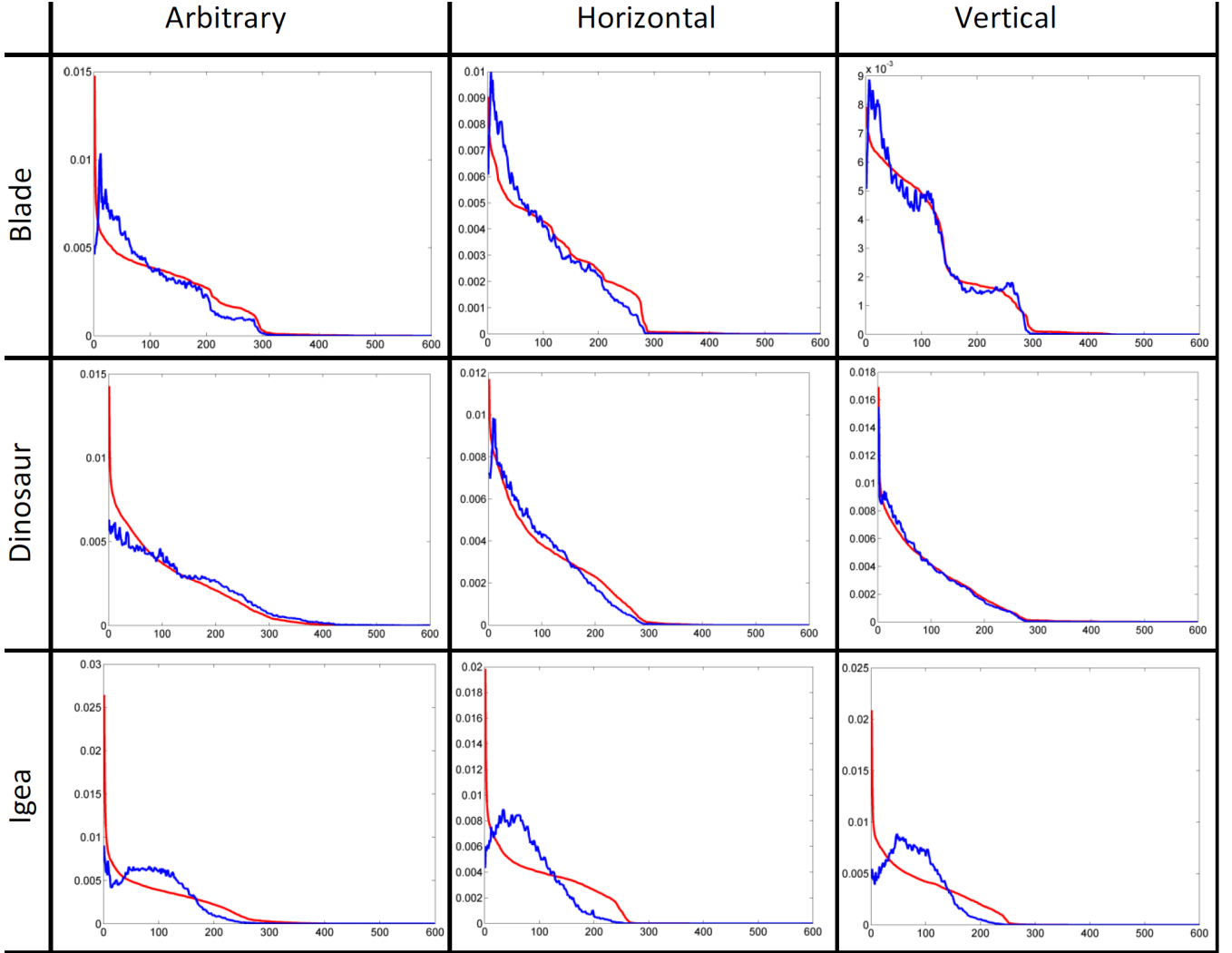


**Figure 2:** Illustration of the influence of disocclusions (i.e., sudden appearance of hidden geometric parts) on human fixations in dynamic scenes. The blue curves represent the distributions of fixation map values with respect to the time during which the vertices are visible to the observers. The red curve is the histogram corresponding to a hypothetical observer looking at all the visible vertices equally. These histograms are shown for each object (Blade, Dinosaur, Igea) and for each camera movement (arbitrary, horizontal, vertical).

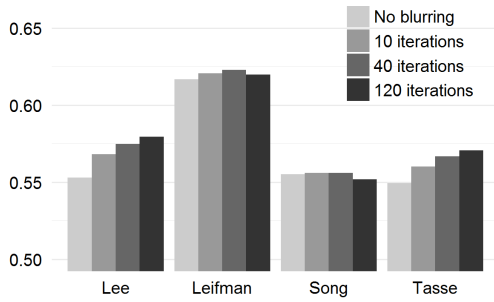


**Figure 3:** Mean AUC values for prediction of Lee [LVJ05], Leifman [LST12], Song [SLMR14] and Tasse [TKD15], according to the level of blurring.

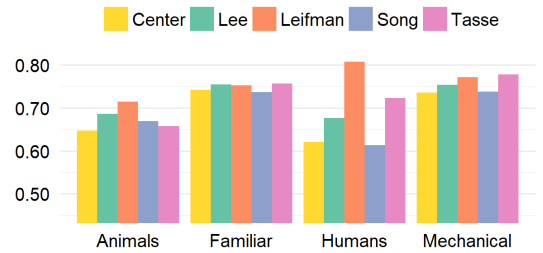


**Figure 4:** AUC values per class for all tested saliency models (combined with center model).

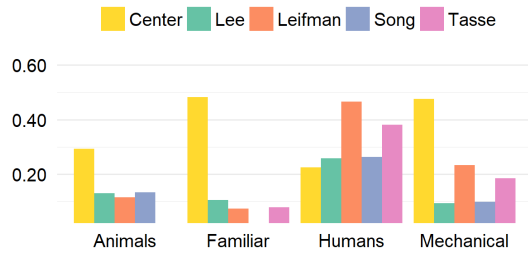


**Figure 5:** Linear correlation values per class for all tested saliency models (not combined with center model).

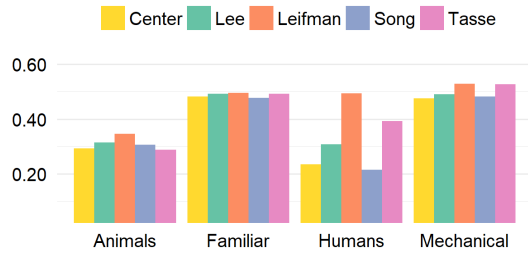


**Figure 6:** Linear correlation values per class for all tested saliency models (combined with center model).

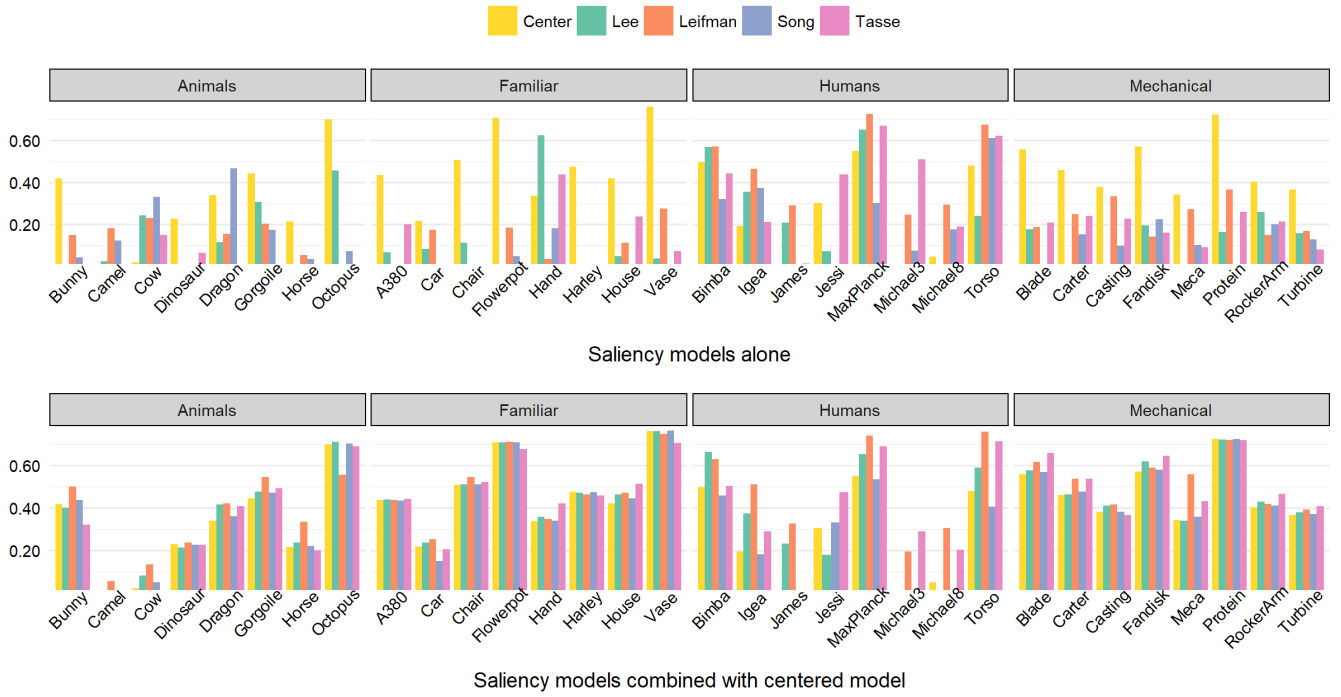


**Figure 7:** Linear correlation values per 3D object for all tested saliency models (alone and combined with center model).

	Center	Leifman	Lee	Tasse		Leifman	Tasse	Lee	Song
<b>Leifman</b>	0.24005	NA	NA	NA	<b>Tasse</b>	0.02421	NA	NA	NA
<b>Lee</b>	0.00212	0.21641	NA	NA	<b>Lee</b>	0.00055	1	NA	NA
<b>Tasse</b>	0.00302	0.04328	1	NA	<b>Song</b>	0	0.00103	0.00013	NA
<b>Song</b>	5e-05	0	0.22771	0.83102	<b>Center</b>	0	6e-05	0.00013	1

**Saliency models alone**

**Saliency models combined with Center**

**Figure 8:** Pairwise *t*-test (Bonferroni-corrected) between all saliency model (computed on AUC values). Methods are ranked from left to right according to their performance in descending order. For each method (on top of each column) we list below the remaining ones with corresponding *p*-values.

	Center	Leifman	Lee	Tasse		Leifman	Tasse	Lee	Center
<b>Leifman</b>	0.00036	NA	NA	NA	<b>Tasse</b>	0.01447	NA	NA	NA
<b>Lee</b>	0	0.05861	NA	NA	<b>Lee</b>	0.00037	1	NA	NA
<b>Tasse</b>	0	0.00743	1	NA	<b>Center</b>	0	0.00098	0.00187	NA
<b>Song</b>	0	0	0.6112	1	<b>Song</b>	0	0.00155	0.00221	1

**Saliency models alone**

**Saliency models combined with Center**

**Figure 9:** Pairwise *t*-test (Bonferroni-corrected) between all saliency model (computed on Linear Correlation values). Methods are ranked from left to right according to their performance in descending order. For each method (on top of each column) we list below the remaining ones with corresponding *p*-values.



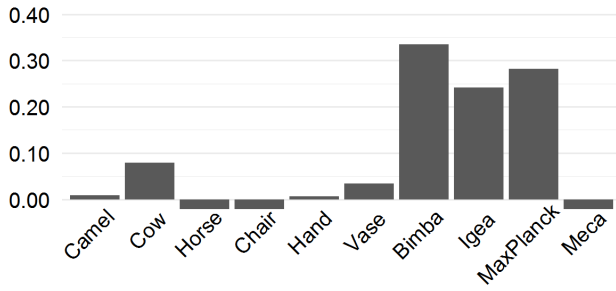


**Figure 10:** Linear correlations between human fixations and Schelling distributions [CSPF12].

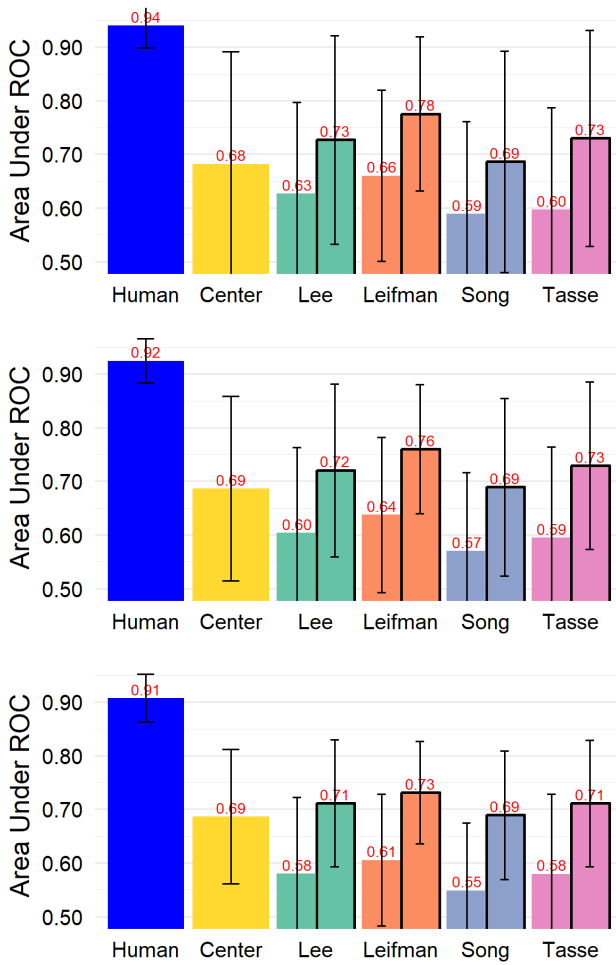


**Figure 11:** Performance, in terms of area under ROC curve of saliency models, for different thresholds. From top to bottom: 10%, 20% and 40%.

#### 4. Fixation and saliency maps

All fixation and saliency maps from experiments 2 are illustrated below.

#### References

- [CSPF12] CHEN X., SAPAROV A., PANG B., FUNKHOUSER T.: Schelling points on 3D surface meshes. *ACM Transactions on Graphics* 31, 4 (jul 2012), 1–12. [5](#)
- [LST12] LEIFMAN G., SHTROM E., TAL A.: Surface regions of interest for viewpoint selection. *Computer Vision and Pattern Recognition* (2012). [2](#), [7](#), [8](#), [9](#), [10](#), [11](#), [12](#), [13](#), [14](#), [15](#), [16](#), [17](#), [18](#)
- [LVJ05] LEE C., VARSHNEY A., JACOBS D.: Mesh saliency. In *ACM Siggraph* (2005), pp. 659–666. [2](#), [7](#), [8](#), [9](#), [10](#), [11](#), [12](#), [13](#), [14](#), [15](#), [16](#), [17](#), [18](#)
- [SLMR14] SONG R., LIU Y., MARTIN R. R., ROSIN P. L.: Mesh Saliency via Spectral Processing. *ACM Transactions on Graphics* 33, 1 (2014). [2](#), [7](#), [8](#), [9](#), [10](#), [11](#), [12](#), [13](#), [14](#), [15](#), [16](#), [17](#), [18](#)
- [TKD15] TASSE F. P., KOSINKA J., DODGSON N.: Cluster-Based Point Set Saliency. *2015 IEEE International Conference on Computer Vision (ICCV)* (2015), 163–171. [2](#), [7](#), [8](#), [9](#), [10](#), [11](#), [12](#), [13](#), [14](#), [15](#), [16](#), [17](#), [18](#)

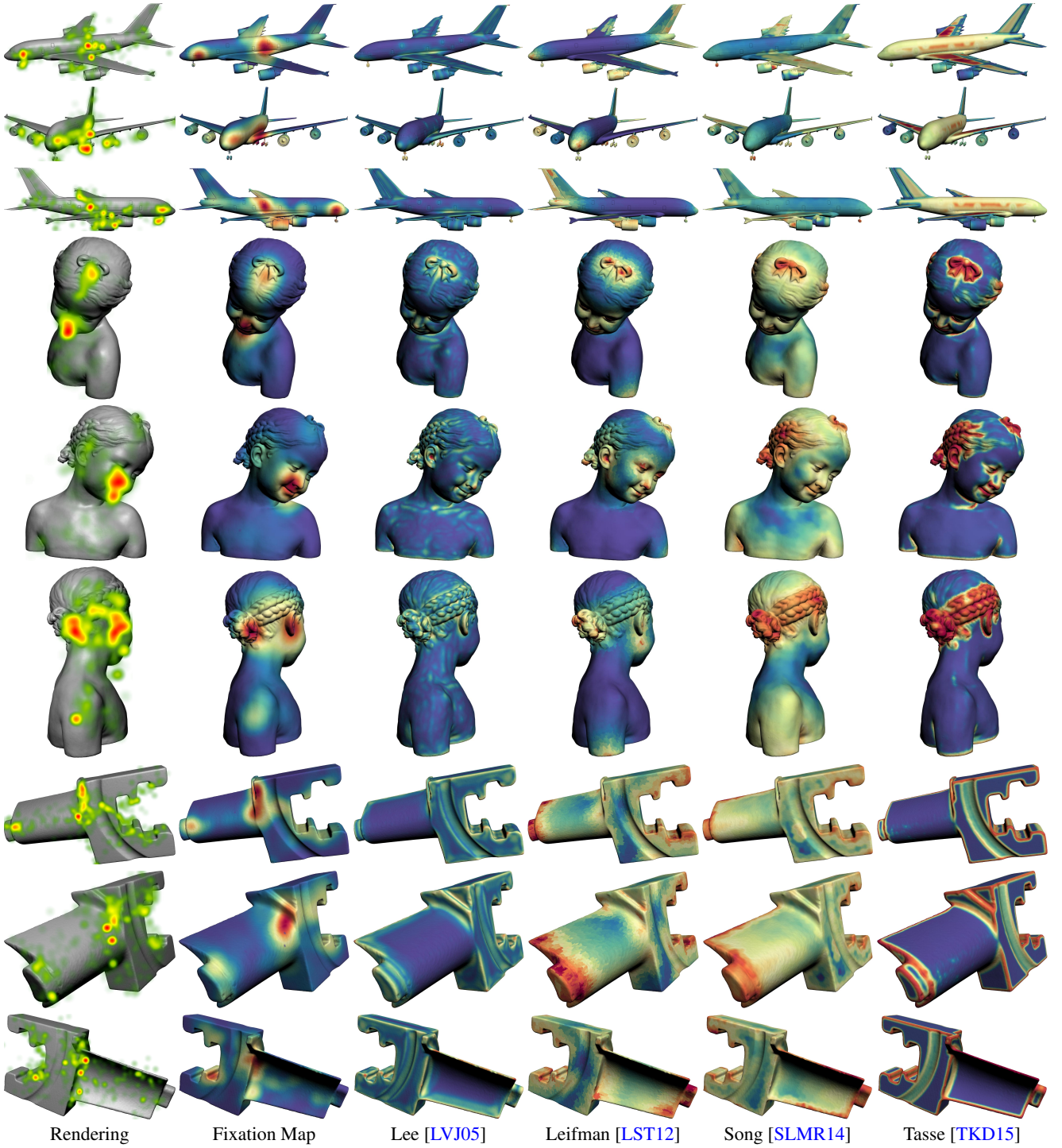


**Figure 12:** Rendering (with 2D heat maps), fixation maps and tested saliency models for several 3D objects. From top to bottom: A380, Bimba and Blade.

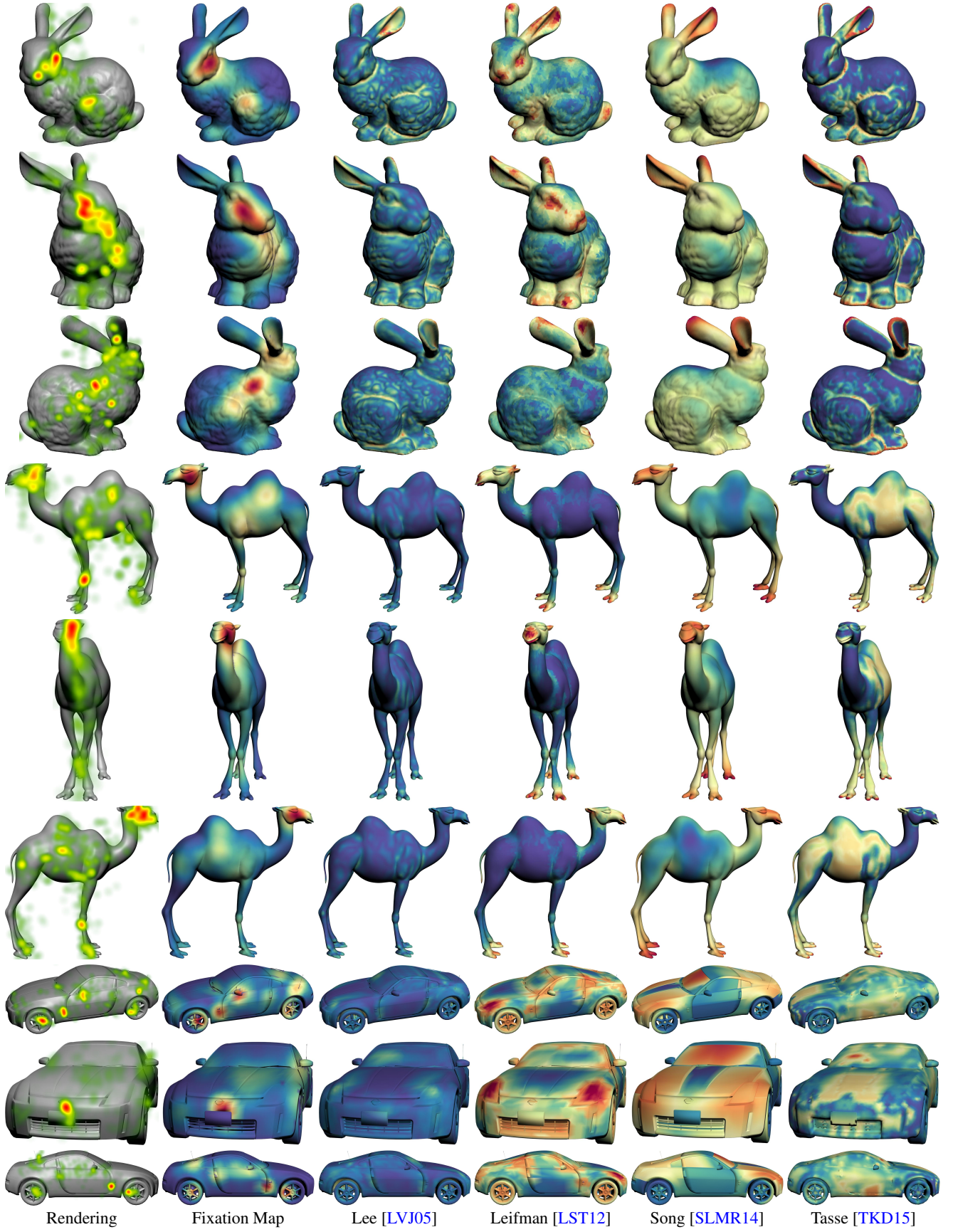


**Figure 13:** Rendering (with 2D heat maps), fixation maps and tested saliency models for several 3D objects. From top to bottom: Bunny, Camel and Car. submitted to EUROGRAPHICS 2018.



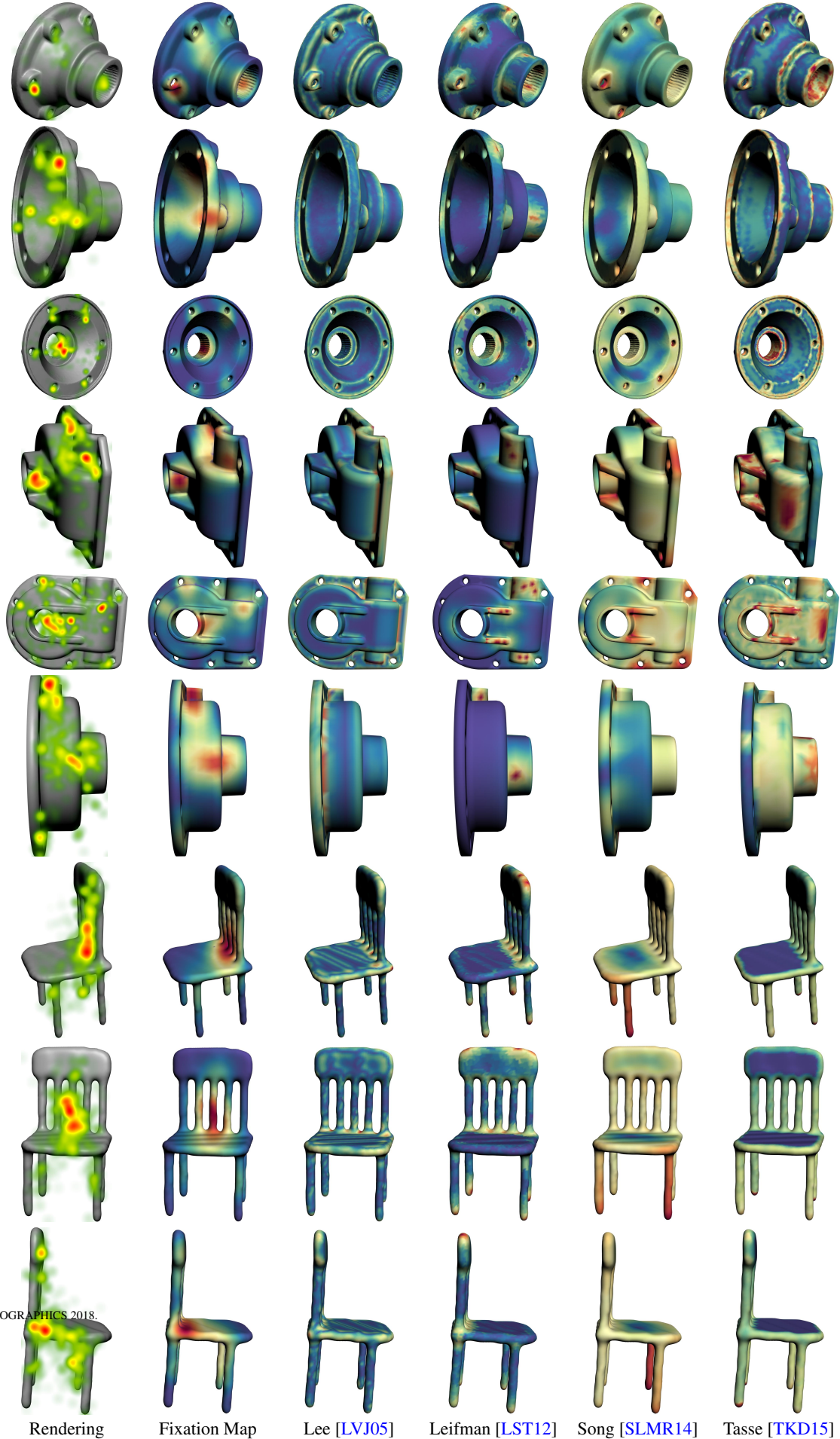


**Figure 14:** Rendering (with 2D heat maps), fixation maps and tested saliency models for several 3D objects. From top to bottom: Carter, Casting and Chair.



**Figure 15:** Rendering (with 2D heat maps), fixation maps and tested saliency models for several 3D objects. From top to bottom: Cow, Dinosaur and Dragon.

submitted to EUROGRAPHICS 2018.



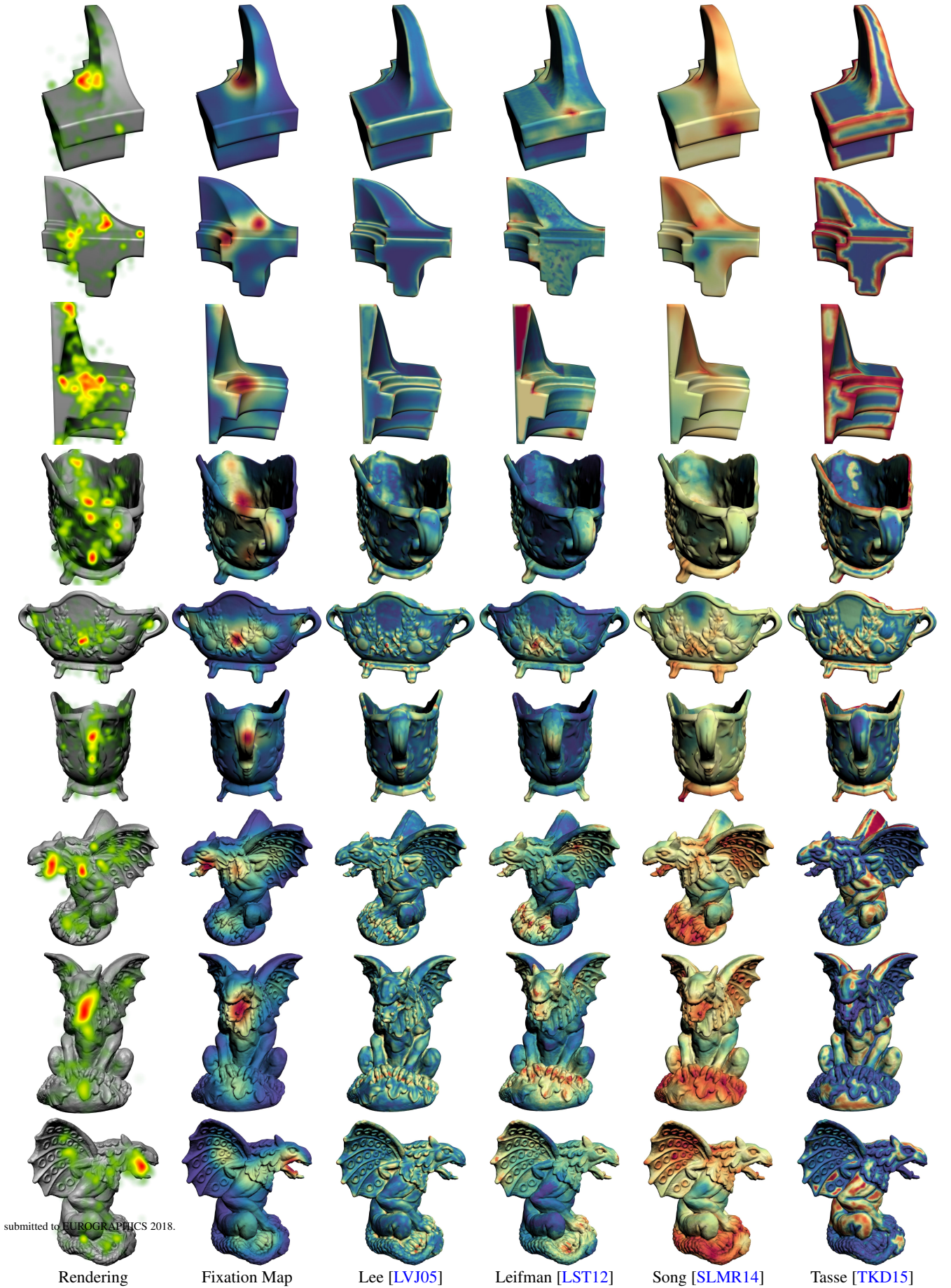


**Figure 16:** Rendering (with 2D heat maps), fixation maps and tested saliency models for several 3D objects. From top to bottom: Fandisk, FlowerPot and Gorgoile.

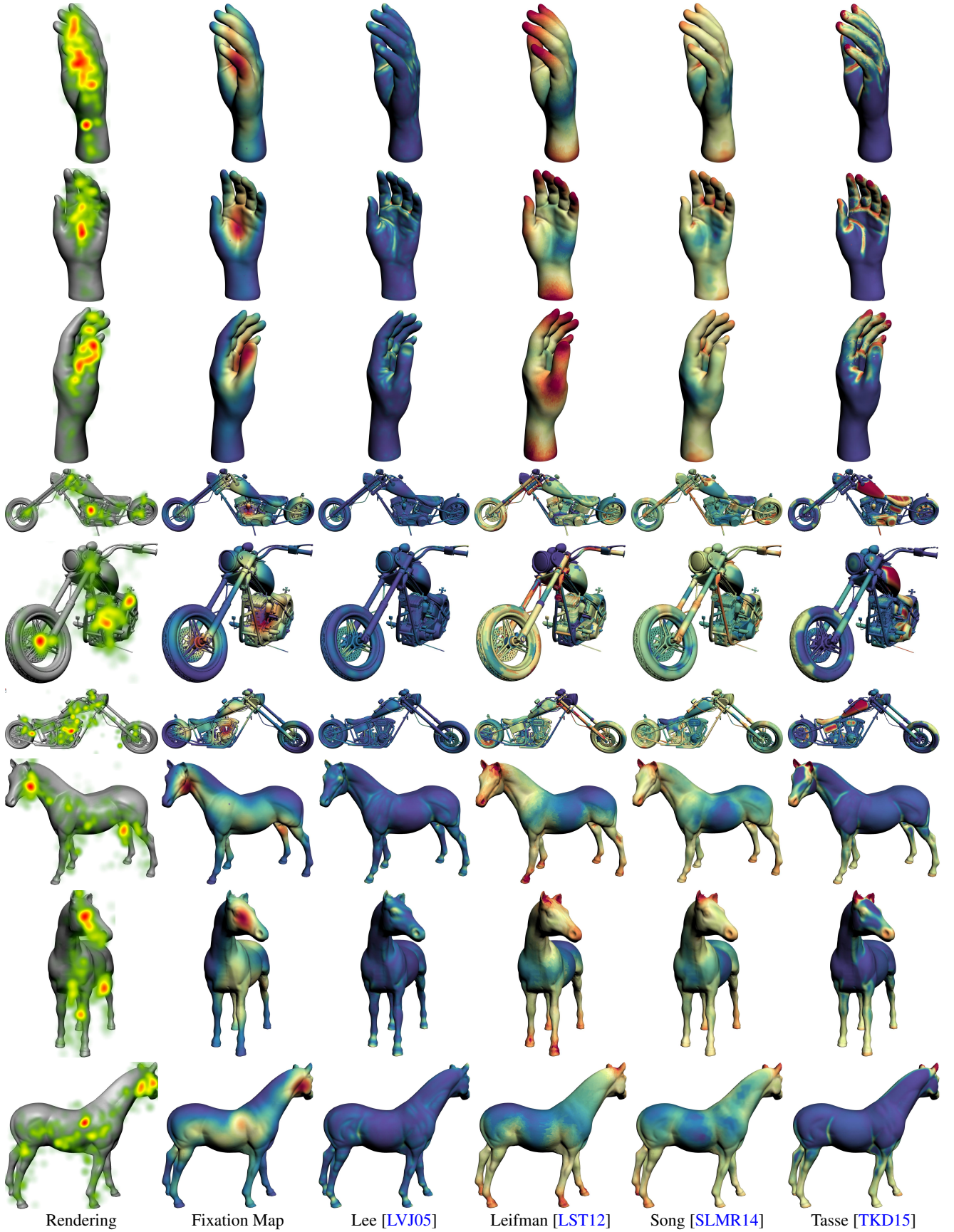
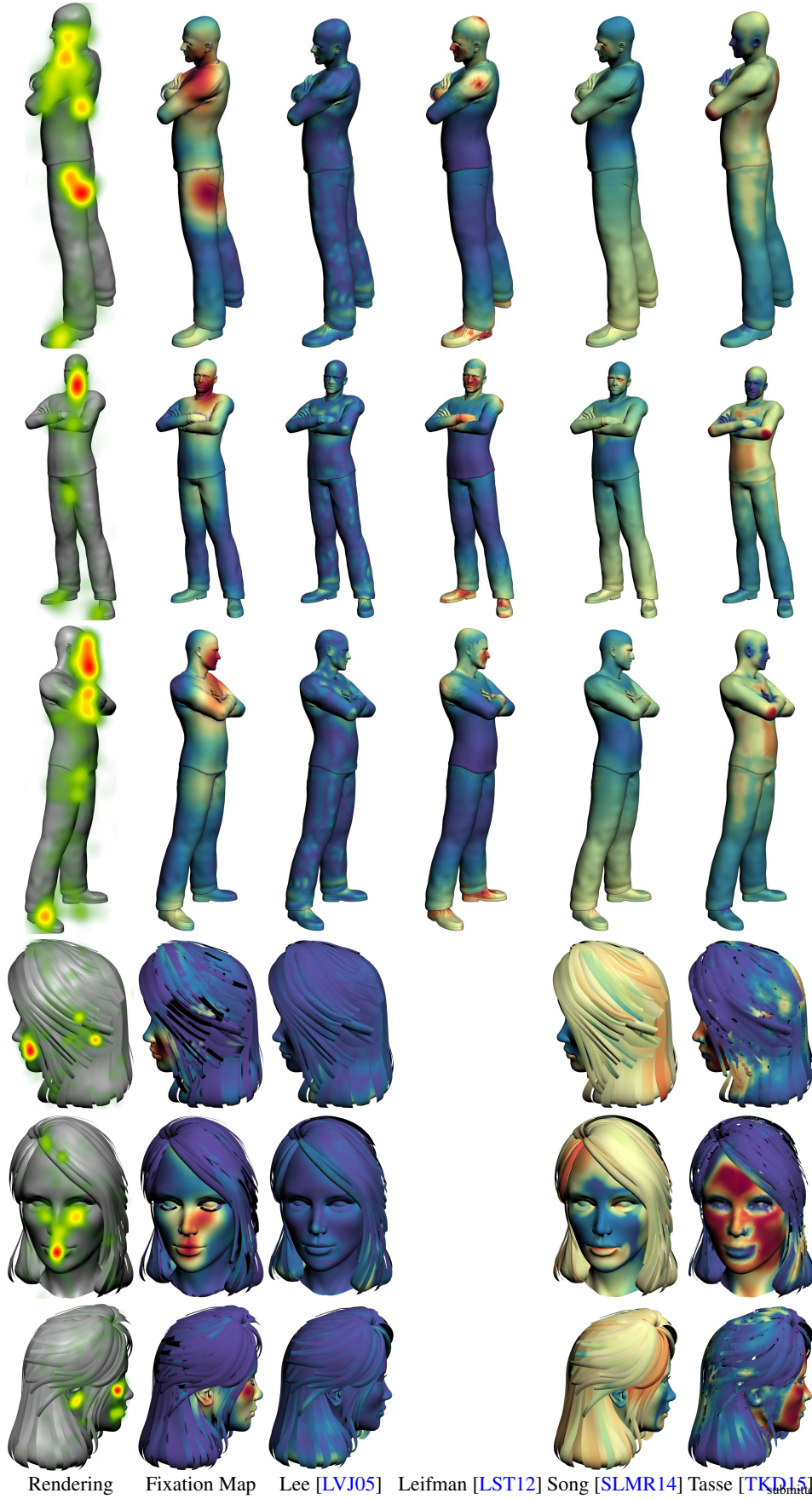


**Figure 17:** Rendering (with 2D heat maps), fixation maps and tested saliency models for several 3D objects. *From top to bottom: Hand, Harley and Horse.*



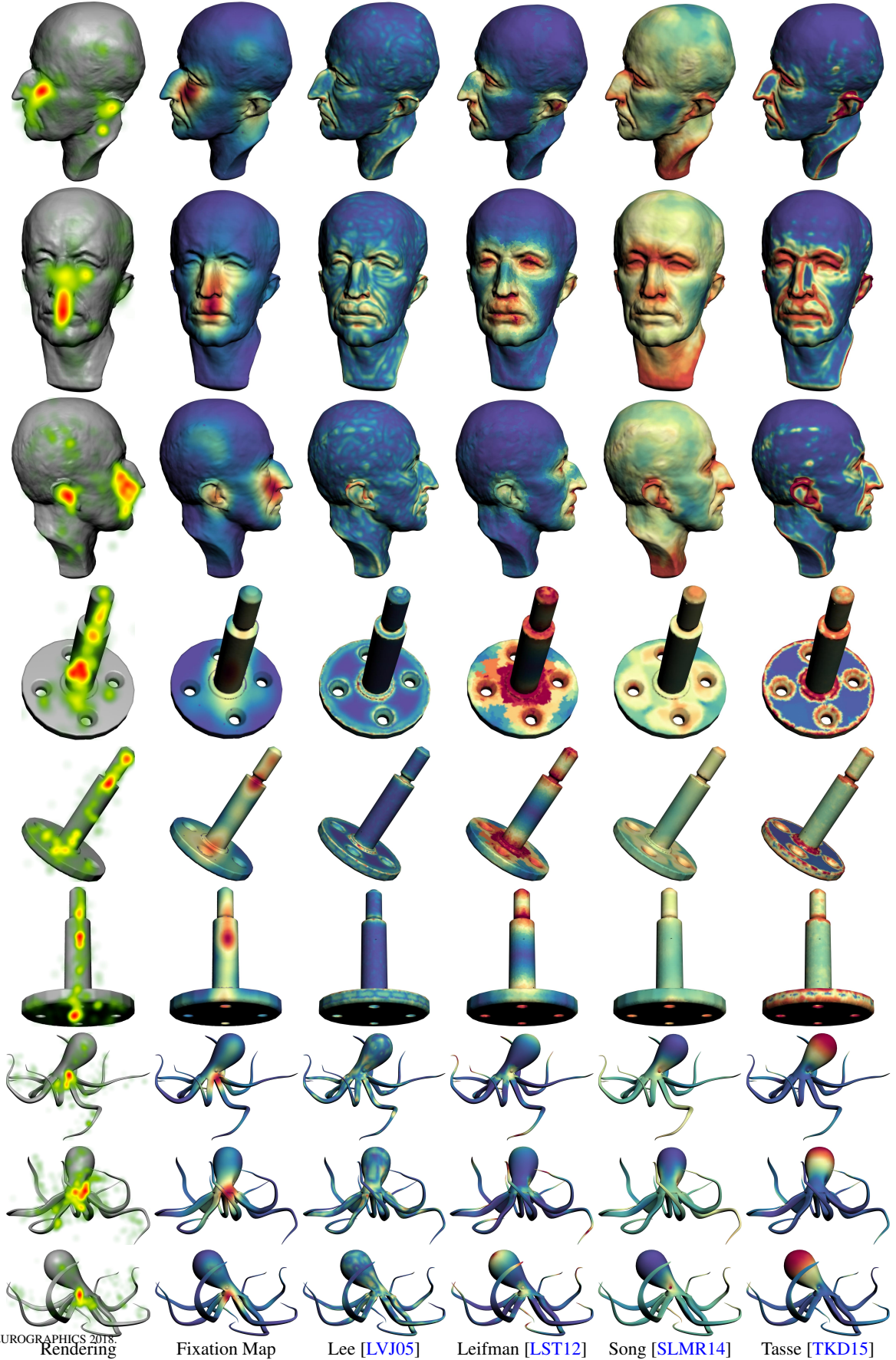


**Figure 18:** Rendering (with 2D heat maps), fixation maps and tested saliency models for several 3D objects. From top to bottom: House and Igea.



**Figure 19:** Rendering (with 2D heat maps), fixation maps and tested saliency models for several 3D objects. From top to bottom: James and Jessi. Note that the algorithm from Leifman et al. did not work for Jessi.



submitted to EUROGRAPHICS 2018.  
Rendering

Fixation Map

Lee [LVJ05]

Leifman [LST12]

Song [SLMR14]

Tasse [TKD15]

**Figure 20:** Rendering (with 2D heat maps), fixation maps and tested saliency models for several 3D objects. From top to bottom: Max-Planck, Meca and Octopus.

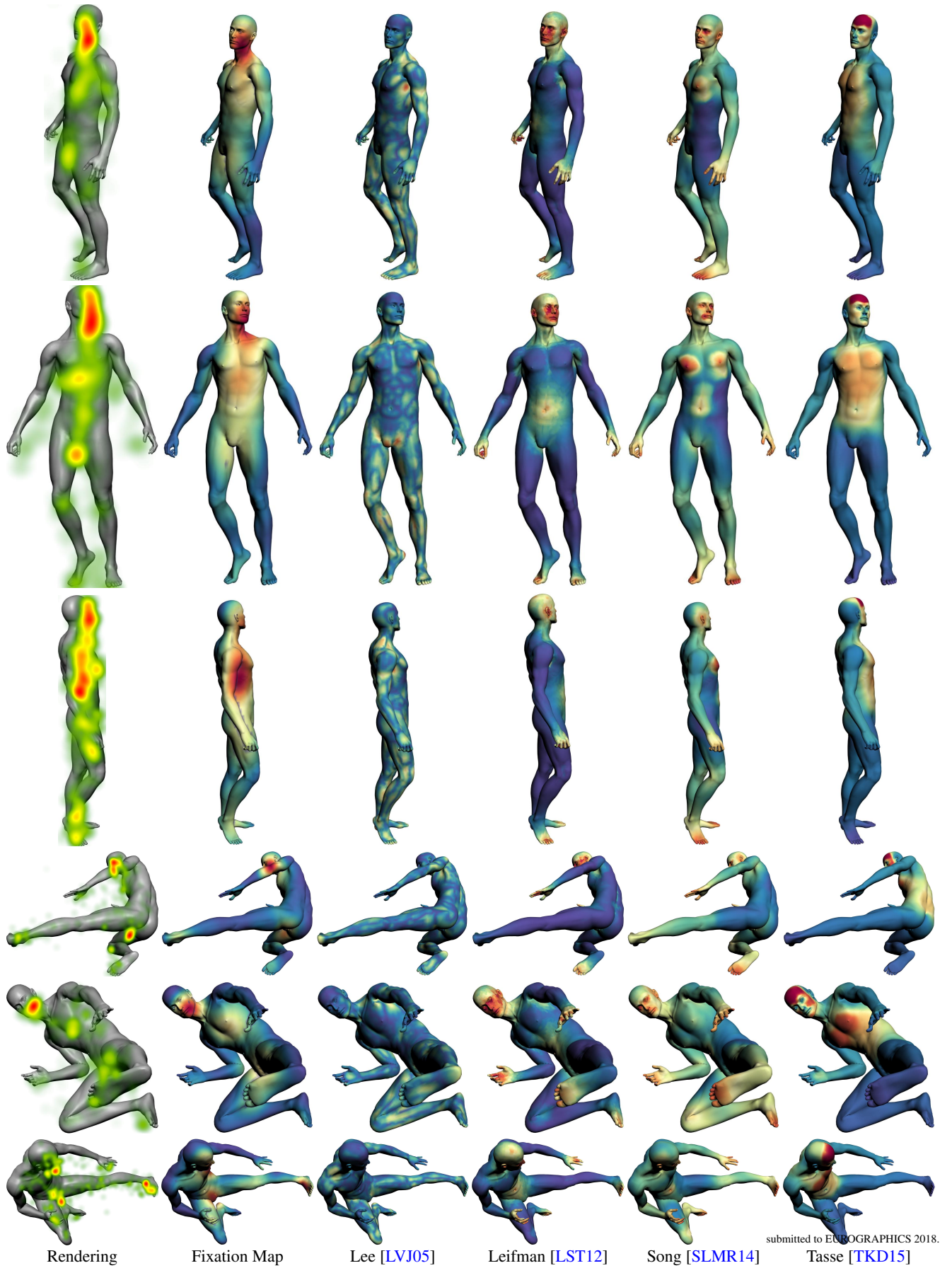


**Figure 21:** Rendering (with 2D heat maps), fixation maps and tested saliency models for several 3D objects. From top to bottom: Michael3 and Michael8.



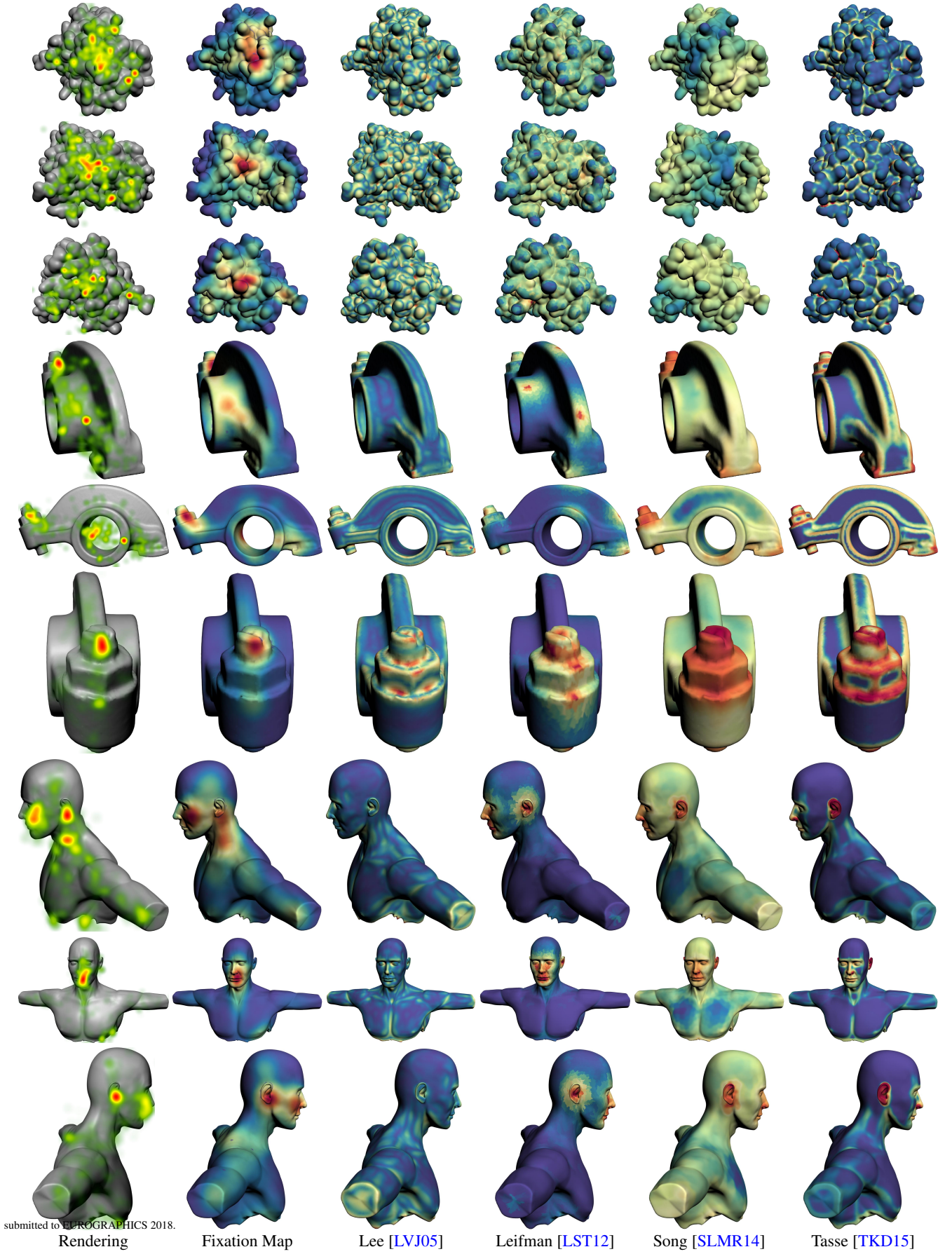


**Figure 22:** Rendering (with 2D heat maps), fixation maps and tested saliency models for several 3D objects. From top to bottom: Protein, RockerArm and Torso.

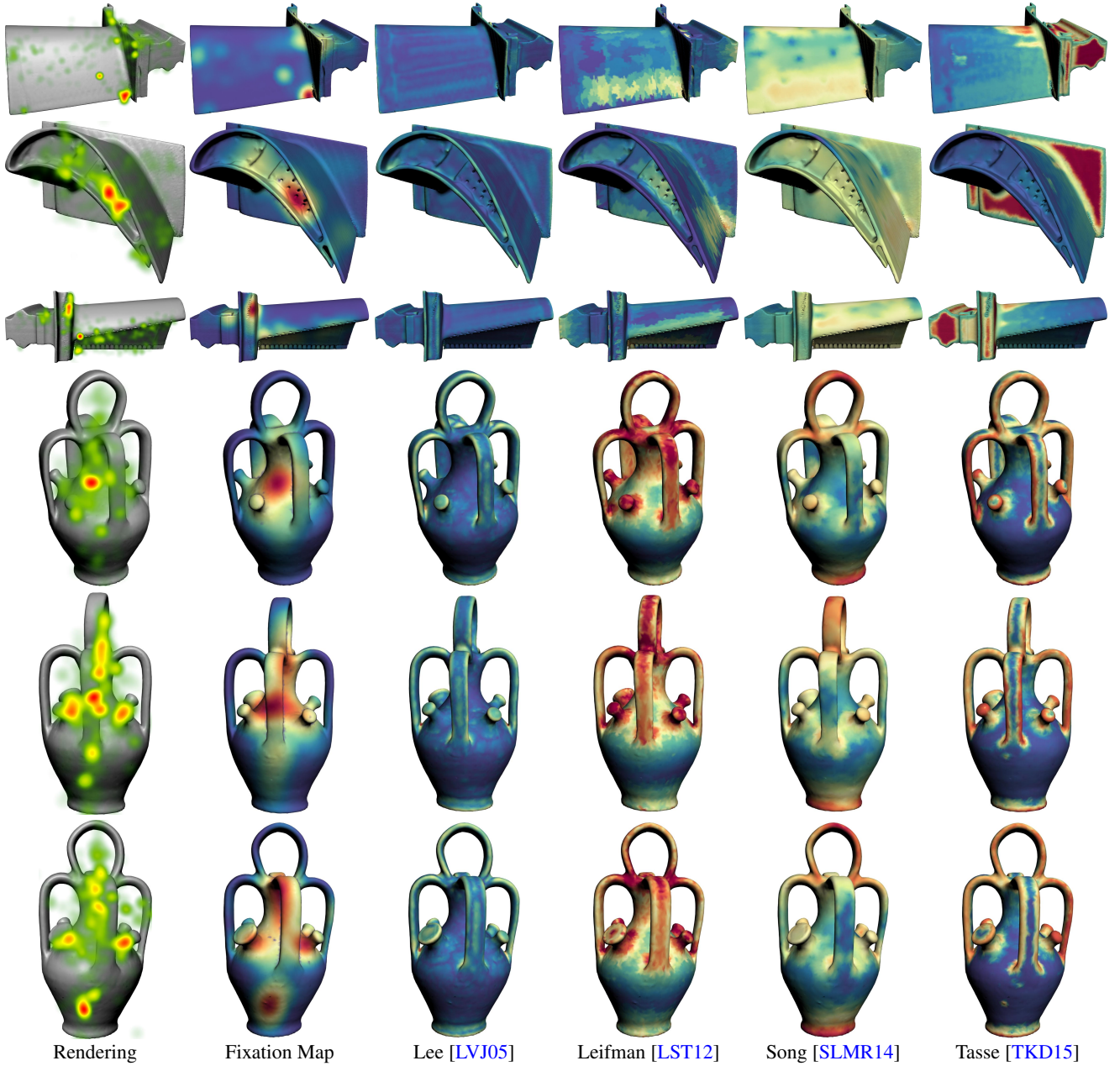


**Figure 23:** Rendering (with 2D heat maps), fixation maps and tested saliency models for several 3D objects. From top to bottom: Turbine and Vase.